The Meteoritical Society

Meteoritics & Planetary Science 43, Nr 8, 1383–1398 (2008)
Abstract available online at http://meteoritics.org

The Dhala structure, Bundelkhand craton, Central India—Eroded remnant of a large Paleoproterozoic impact structure

Jayanta K. PATI[1], Wolf Uwe REIMOLD[2*], Christian KOEBERL[3], and Puniti PATI[1]

[1]Department of Earth and Planetary Sciences, Nehru Science Centre, University of Allahabad, Allahabad-211 002, India
[2]Museum for Natural History, Humboldt University in Berlin, Invalidenstrasse 43, 10115 Berlin, Germany
[3]Center for Earth Sciences, University of Vienna, Althanstasse 14, A-1090, Vienna, Austria
[*]Corresponding author: E-mail: uwe.reimold@museum.hu-berlin.de

(Received 31 July 2007; revision accepted 10 March 2008)

Abstract–The newly discovered Dhala structure, Madhya Pradesh State, India, is the eroded remnant of an impact structure with an estimated present-day apparent diameter of about 11 km. It is located in the northwestern part of the Archean Bundelkhand craton. The pre-impact country rocks are predominantly granitoids of ~2.5 Ga age, with minor 2.0–2.15 Ga mafic intrusive rocks, and they are overlain by post-impact sediments of the presumably >1.7 Ga Vindhyan Supergroup. Thus, the age for this impact event is currently bracketed by these two sequences. The Dhala structure is asymmetrically disposed with respect to a central elevated area (CEA) of Vindhyan sediments. The CEA is surrounded by two prominent morphological rings comprising pre-Vindhyan arenaceous-argillaceous and partially rudaceous metasediments and monomict granitoid breccia, respectively. There are also scattered outcrops of impact melt breccia exposed towards the inner edge of the monomict breccia zone, occurring over a nearly 6 km long trend and with a maximum outcrop width of ~170 m. Many lithic and mineral clasts within the melt breccia exhibit diagnostic shock metamorphic features, including multiple sets of planar deformation features (PDFs) in quartz and feldspar, ballen-textured quartz, occurrences of coesite, and feldspar with checkerboard texture. In addition, various thermal alteration textures have been found in clasts of initially superheated impact melt. The impact melt breccia also contains numerous fragments composed of partially devitrified impact melt that is mixed with unshocked as well as shock deformed quartz and feldspar clasts. The chemical compositions of the impact melt rock and the regionally occurring granitoids are similar. The Ir contents of various impact melt breccia samples are close to the detection limit (1–1.5 ppb) and do not provide evidence for the presence of a meteoritic component in the melt breccia. The presence of diagnostic shock features in mineral and lithic clasts in impact melt breccia confirm Dhala as an impact structure. At 11 km, Dhala is the largest impact structure currently known in the region between the Mediterranean and southeast Asia.

INTRODUCTION

There are currently 171 (Earth Impact Database 2008; NB: the two Arkenu 1 and 2 structures listed as well are not considered by us as confirmed impact structures! See Reimold 2007) impact structures known on Earth, but the well-studied, 1.8 km in diameter Lonar structure (e.g., Fredriksson et al. 1973; Osae et al. 2005) in Maharashtra (central India) is until now the only confirmed impact structure in the entire region of the Indian subcontinent and Far East Asia. Besides Lonar, the so-called Ramgarh structure, an ~4 km wide crater-like feature in Rajasthan (Master and Pandit 1999; Sisodia et al. 2006), and the proposed Shiva structure in the Arabian Sea to the southwest of the Indian subcontinent (Chatterjee et al. 2006), have been suggested as being of possible impact origin. However, Chatterjee et al. (2006) do not provide any tangible evidence for the existence of a crater structure and certainly not for the existence of an impact structure at Shiva. The Ramgarh structure has not yet yielded bona fide impact evidence either (Reimold et al. 2006).

Here, we report the discovery and confirmation of a new large impact structure, the Dhala structure, centered at 25°17′59.7″N and 78°8′3.1″E in the western part of the Archean Bundelkhand craton, in the Shivpuri District of Madhya Pradesh State of India. The first reports of the

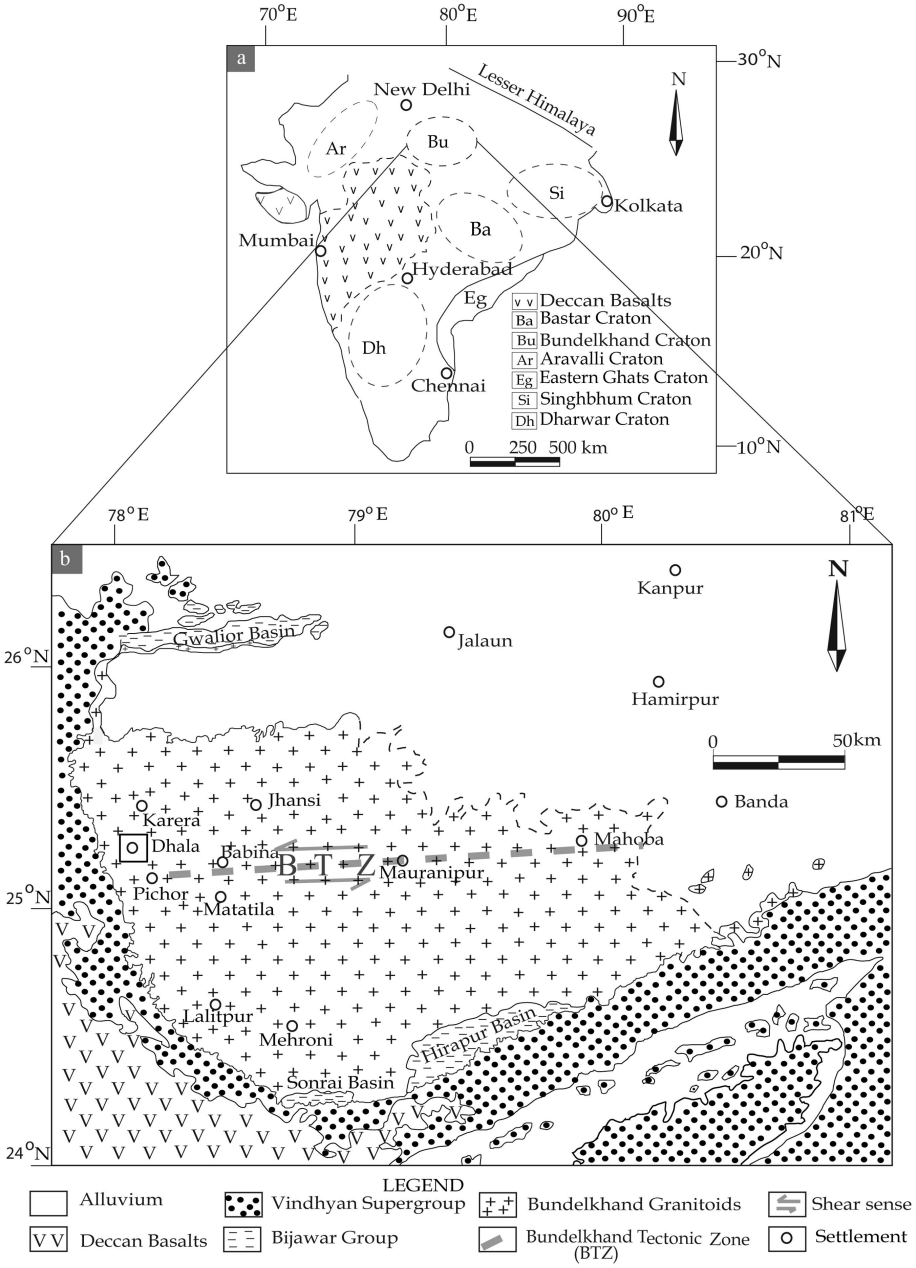

Fig. 1. a) The various cratonic blocks of India are shown schematically on a map of India: The Bundelkhand craton (Bu), Aravalli craton (Ar), Singhbhum craton (Si), Dharwar craton (Dh), Eastern Ghats craton (Eg), and Baster craton (Ba) are the main cratonic blocks of Archean age. b) A simplified geological map of the Bundelkhand craton shows the location of the Dhala structure (encircled) and the regional geology. Adapted from Pati et al. (2007) The rectangle around the symbol for Dhala village indicates the area of the geological map shown in Fig. 3.

existence of the structure and its origin by impact were made in abstract form by Pati (2005) and Pati et al. (2006).

GEOLOGIC SETTING OF THE BUNDELKHAND CRATON

The Bundelkhand craton is one of four Archean shields (Dharwar, Singhbhum, Aravalli, and Bundelkhand) in India (Fig. 1a). The Bundelkhand shield occupies nearly 29,000 km^2 in the Central Indian Shield region (Fig. 1b); it consists of supracrustal gneisses with or without tonalite-trondhjemite-granodiorite (TTG) affinity, metapelites, amphibolites, iron-rich and, less abundantly, manganese-rich metasedimentary rocks, marble, calc-silicate rocks and quartzites. Several phases of compositionally different felsic intrusive rocks, felsic volcanic rocks, giant quartz veins (GQVs) (Pati et al. 2007), and mafic-ultramafic intrusive rocks (Basu 1986; Mondal et al. 2002; Malviya et al. 2006) are also present. The giant quartz veins are up to 70 m wide and can exceed 100 km in strike length, and are the most conspicuous regional

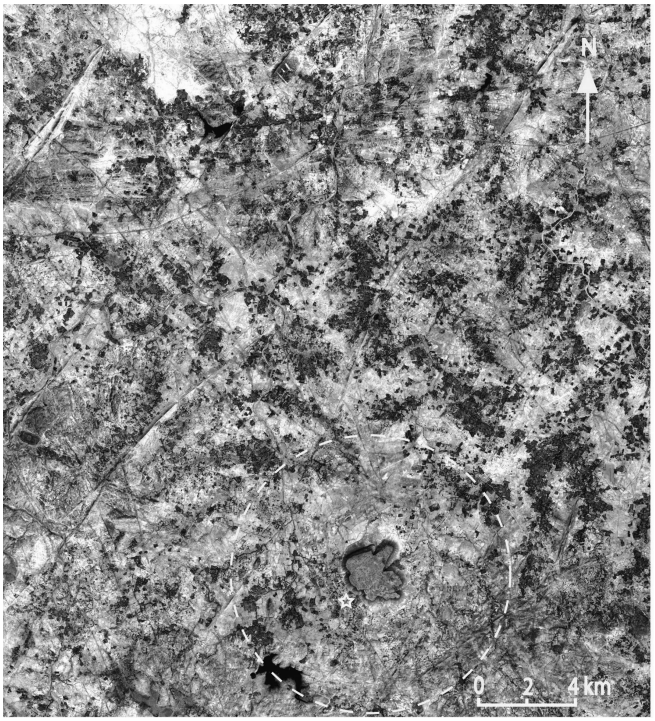

Fig. 1. *Continued*. c) Indian Remote Sensing satellite (IRS-1) image of the region around the Dhala structure, acquired on 22 February 2003. The image is centered at N25°22′53″/E78°7′42″and the width of the area shown is 26 km. The impact structure perimeter is enhanced by a dashed white line. Only the flat-topped, sediment-covered, central (although off-center) elevated area stands out clearly in this image, just northeast of Dhala village (star symbol).

structures observed as curvilinear features throughout the Bundelkhand craton. These veins were later intruded by NW-trending mafic dikes. The supracrustal gneisses show three phases of folding and the imprint of a crustal-scale brittle-ductile shearing (~E-W trending) episode that affected all major lithologies except the mafic dikes (Malviya et al. 2006; Pati et al. 2007). The Bundelkhand rocks, in general, are metamorphosed to amphibolite facies (Basu 1986) and, in places, possibly to granulite facies (J. K. Pati, unpublished data).

GENERAL GEOLOGY OF THE DHALA AREA

The deeply eroded Dhala structure is hardly visible in Landsat (TM), Shuttle Radar Topography Mission (SRTM), and Indian Remote Sensing Satellite (IRS)-1D hybrid [Linear Image Scanning System, (LISS)-III + Panchromatic (PAN)] images (e.g., Fig. 1c). Off-center to the outline of the structure occurs a 426 m high, mesa-shaped hill, 2.5 km in diameter, to the northeast of Dhala village (Fig. 1c). The Dhala structure occupies nearly 64 km^2 some 50 km WSW of the town of Jhansi, Uttar Pradesh State, India (Fig. 1b). A number of roughly southwest-northeast to east-west trending linear to curvilinear GQVs with positive relief (up to 380 m high) are observed on the eastern, western and southern sides of the structure. The present-day apparent (cf. discussion in Turtle et al. 2005) diameter of the structure is estimated at 11 km on the basis of the mapped distribution of monomict impact breccia (see below: breccia discussion). The maximum elevation in the Dhala area has been recorded at the top of the central hill (the background feature in Fig. 2) and the minimum elevation (295 m) near Bhaunti (~4 km northwest of Dhala village) in the vicinity of the Paronch River. A weakly defined, annular drainage pattern in the vicinity of the CEA is observed on a topographic map (Survey of India topographic sheet no. 54K/3; 1:50,000).

The Dhala area mainly comprises calc-silicate rocks, granitoids (including TTG lithologies), very large quartz veins (GQV), and dolerites, as well as sandy siltstone-siltstone with conglomerate lenses and an intercalated shale-sandstone unit with a small exposure of bedded ash and laterite occurring on the top of the central hill, which is partly covered by Quaternary alluvium.

Based on earlier field, petrological and geophysical data, the Dhala structure has traditionally been referred as a "cauldron structure" (Jain et al. 2001; Srivastava et al. 2002; Shrivastava and Nambiar 2003; Rao et al. 2005). Besides a cryptovolcanic origin, it has also been suggested that "intense rotational movement" of "micro-brecciated granite" led to the development of this "circular feature at Mohar" (Basu 2004). The area was drilled recently by the Geological Survey of India (Central Region) and the Atomic Mineral Division (Government of India) after some preliminary indications of radioactive minerals had been reported. However, the drilling results are not yet available in the public domain.

Based on gravity, magnetic, and electrical resistivity surveys in parts of the Dhala structure, Rao et al. (2005) concluded that this "ring structure" represented a confirmed cauldron. Their gravity map shows an ENE-WSW trending, 1 to 2 mgal negative anomaly in the central part of the structure. In addition, they interpreted resistivity data from the central part of the structure to indicate that a depression in the basement rocks was overlain by 400–500 m of sediments.

GEOLOGY OF THE DHALA STRUCTURE

The regional geological map (Fig. 3; modified after Srivastava and Nambiar 2003) shows the litho-tectonic situation in the Dhala area. The Dhala structure is a near-circular feature with three distinct morpho-lithological domains. The most prominent one is the central elevated area (CEA; about 5 km^2), comprising a sequence of alternating sub-horizontal sandstone-pebbly sandstone and shale with small exposures of lateritized conglomerate (~1600 Ma or less; pre-Kaimur Formation, Vindhyan Supergroup, Srivastava et al. 2002) and bedded ash. The ash occurs as a small exposure (20 × 18 m^2) of variegated, thinly bedded, and unconsolidated material in the vicinity of the conglomerate horizon. However, its relationshipwith the regional and local geology is unknown. The CEA is surrounded by a nearly circular ring covering, on

Fig. 2. The mesa-like structure in the central elevated part of the Dhala structure can be observed from a distance with an extensive breccia exposure in the foreground. The low-lying area in between is covered by sandy siltstone-siltstone (pre-Vindhyan sediments) overlain by alternating argillaceous-arenaceous sediments (Vindhyan Supergroup).

aggregate, about 16 km^2 comprising mainly flat-lying, intercalated purplish-brown siltstone and greenish-white sandy siltstone, with local polymict conglomerate lenses that contain clasts of chert, jasper, and quartz in a clastic matrix. Slump structures and contorted bedding are also observed within this litho-unit, especially close to the CEA. Large angular clasts of granitoids (centimeter to >2 m size) similar to drop-stones possibly derived from a proximal source are also observed. These sediments are overlain by Vindhyan Supergroup rocks.

The outermost annular zone of the Dhala structure (Fig. 3) covering 43 km^2 is composed of a monomict breccia unit (earlier called "collapse breccia;" Srivastava et al. 2002; Shrivastava and Nambiar 2003) with varied topographic expressions from its inner to outer margin. One hundred and fourteen breccia outcrops have been observed in this breccia ring. The inner portion comprises a hilly terrain with characteristically whaleback-like outcrops with elevations between 334 and 302 m. The outer rim of the breccia ring constitutes comparatively low lying areas (300 ± 5 m elevation). The essentially monomict breccia comprises fractured and extensively brecciated country rock (predominantly granitoids). Especially in the outer part of this zone, the breccia is largely covered by alluvium. The areal extent of monomict breccia exposures varies from <1 to more than 100 m.

Towards the inner margin and within the breccia ring, seven patchy outcrops of a distinct melt breccia (Fig. 3) occur between 1.9 km NW of Dhala village and 1 km SW of Maniar village (78°2′18″E, 25°2′42″N) over a trend length of nearly 6 km in a semi-circular pattern. These outcrops were earlier designated as "felsic volcanics" occurring as "linear bodies" by Srivastava et al. (2002). The exposures range in width from 7 to 169 m and in length from 15 to 446 m.

The GQVs, thought to possibly be of hydrothermal origin (Pati et al. 2007), occupy mostly north-northeast to north trending fractures through the basement granitoids. They are not related to the formation of the Dhala structure, but are part of the basement. The mafic dikes cut across the regional granitoids with a preferential northwest-southeast trend and displaying sharp contacts. These mafic rocks are extensively altered and fractured. The linear outcrop pattern observed in the case of mylonitized diorite, giant quartz veins, and mafic dikes is overprinted within a 3 km wide area around the central hill by extensive brittle deformation and displacements by up to 200 m from the respective regional trends. Displacement vectors trend radially away from the CEA.

MESOSCOPIC STRUCTURES OF THE DHALA AREA

The geological structure of the actual Dhala area is different from that in the rest of the Bundelkhand craton. Five phases of deformation (three phases of folding and two phases of shearing; Prasad et al. 1999) have been reported from different parts of the Bundelkhand craton to have occurred during the Precambrian. In the Dhala area, a primary fabric is well developed in calc-silicate rocks in the

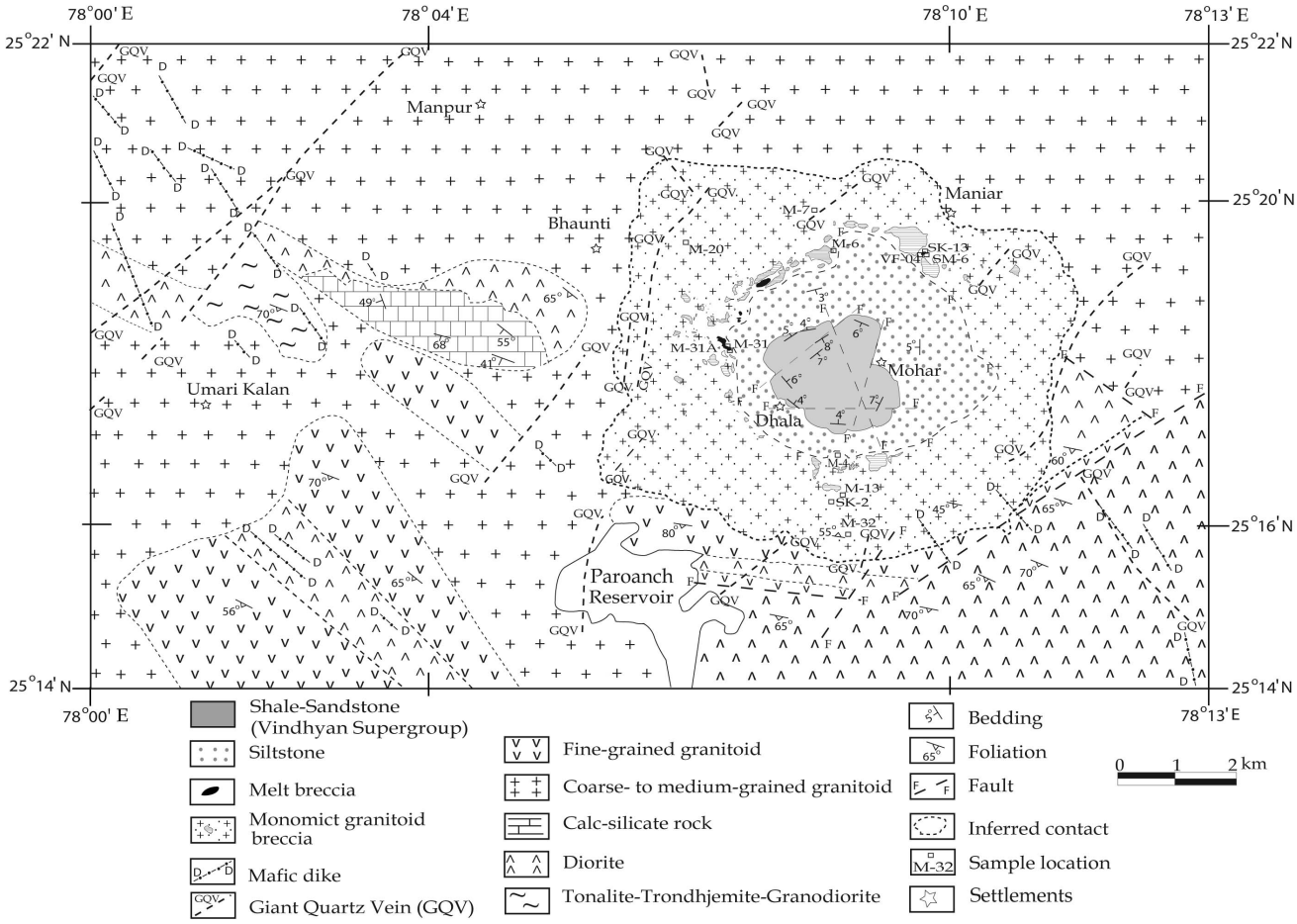

Fig. 3. The geological map of the Dhala area (modified after Jain et al. 2001) exhibits a roughly circular feature (Central Elevated Area [CEA]), surrounded by a broad monomict granitoid breccia ring and sub-horizontally disposed Vindhyan sediments in the environs of the CEA. The flat-lying area in between comprising sandy siltstone and siltstone shows asymmetric outcrop patterns similar to the occurrence of the breccia exposures. North is up.

form of an approximately east-west trending pattern of felsic and mafic compositional layering, with moderate to subvertical dips. Calc-silicate rocks in the Dhala area only preserve the signatures of the first phase of folding (Fig. 4). The early subvertical, open folds show northwest-southeast to east-west trending axial planes with southwesterly to southerly dips, respectively. However, due to extensive fracturing and tilting of strata, the original tectonic setting of these folded rocks could not be determined with confidence during the present study. The mylonitized diorite occurring to the south of the Dhala structure exhibits a prominent east-west trending planar fabric with steep dips to the south, whereas diorites exposed to the southwest of Bhaunti (northeast of Dhala village, compare Fig. 3) show moderate dips. The medium- to fine-grained granitoids show a roughly east-west trending mylonitic foliation with southerly subvertical dips.

Except for the alluvium and the cover sediments (Vindhyan Supergroup), all other rock types are highly fractured with random fracture/joint orientations. The GQVs (Pati et al. 2007) show brecciation on the outcrop scale, and the curvilinear ridges are displaced perpendicular to their strike direction. The sense of displacement is both sinistral and dextral, and the direction of displacement is radial with respect to the central elevated area. Similar displacements are observed in cases of mesoscopic quartz veins occurring in outcrops of the monomict lithic breccia. A number of faults parallel to northeast-southwest trending giant quartz veins, and some others with north-south to north-northwest—south-southwest orientations, are also observed on the mesoscopic scale and as regional features visible on satellite images. Concentric faults seemingly surround the structure at distances of about 0.5 to 1.5 km outside of the central elevated feature. The central elevated feature is also traversed by a number of regional faults trending in E-W, NE-SW, NNE-SSW, and NNW-SSE directions.

Both joint and fault orientations show a radial pattern with possible reactivation of some paleo-fractures that follow the regional trends of giant quartz veins and mafic dikes. The long axes of granitoid clasts measured on monomict lithic breccia outcrops display random orientation (Fig. 5; Pati et al. 2006). The cover sediments (Vindhyan

Fig. 4. The calc-silicate rocks occurring to the NW of the CEA preserve the first phase of folding on a bedding surface distinguished on the basis of color banding, grain size, and compositional variation.

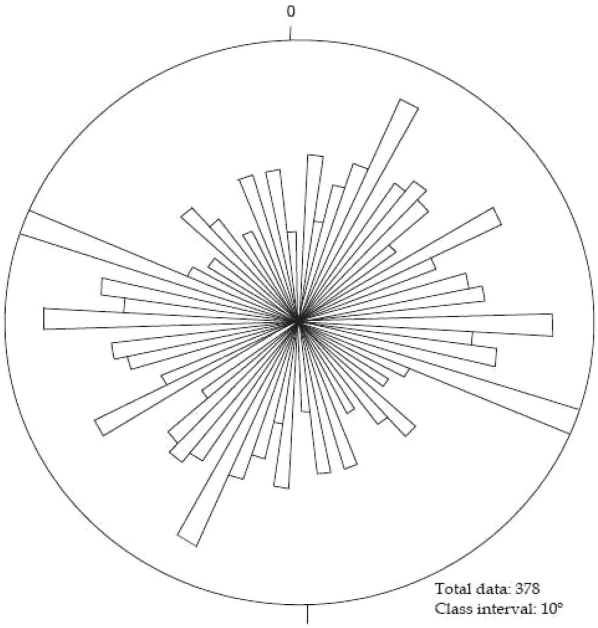

Fig. 5. Long axis trend of 378 granitoid clasts measured at 114 monomict breccia outcrops shows a random distribution. The Rose diagram has been plotted with a 10º class interval.

Supergroup) and the underlying purplish-brown sandy siltstone-siltstone unit with polymict conglomerate pockets also contain syn-sedimentary deformation structures, such as slump folds and contorted lamination. These strata show mostly dips pointing towards the center of the CEA (compare Fig. 3).

PETROGRAPHY

The rocks exposed in the Dhala area can be subdivided based on their relative ages and some geochronological data for similar rocks from nearby localities. Thus, rocks that pre-date the formation of the Dhala structure, those that are related to it, and those that post-date it can be distinguished. The pre-Dhala rocks include all granitoids mentioned, the calc-silicate rocks, vein quartz, diorites, and dolerites. The fractured/brecciated granitoids and the melt breccia constitute the syn-Dhala litho-types. The siltstone with conglomerate lenses and Vindhyan sediments (pebbly sandstone, conglomerate, sandstone, and shale) exposed in the central elevated area constitute post-Dhala rock types.

The pre-Dhala, texturally varied granitoids, calc-silicate rocks, vein quartz, and mafic dike rocks occurring in the Dhala area are all altered to various degrees. The granitoids show porphyritic texture with alkali feldspar phenocrysts and contain K-feldspar, quartz, ± perthite, plagioclase (Ab-rich; oligoclase-andesine), ± hornblende, ± biotite, zircon, apatite, sphene, magnetite, ± calcite, ± chlorite, ± epidote, and ± tourmaline. The calc-silicate rock shows alternate light green and dark grey colored bands of mm to cm thicknesses in the form of a prominent primary fabric defined by the alignment of amphibole (hornblende-tremolite). These rocks are generally altered, which is expressed by iron oxide leaching and elephant-skin weathering on the outcrop. The calc-silicate is composed of amphibole, K-feldspar, quartz, diopside, apatite, calcite, ± wollastonite. The diorite is dark grey, is composed of plagioclase, microcline, hornblende,

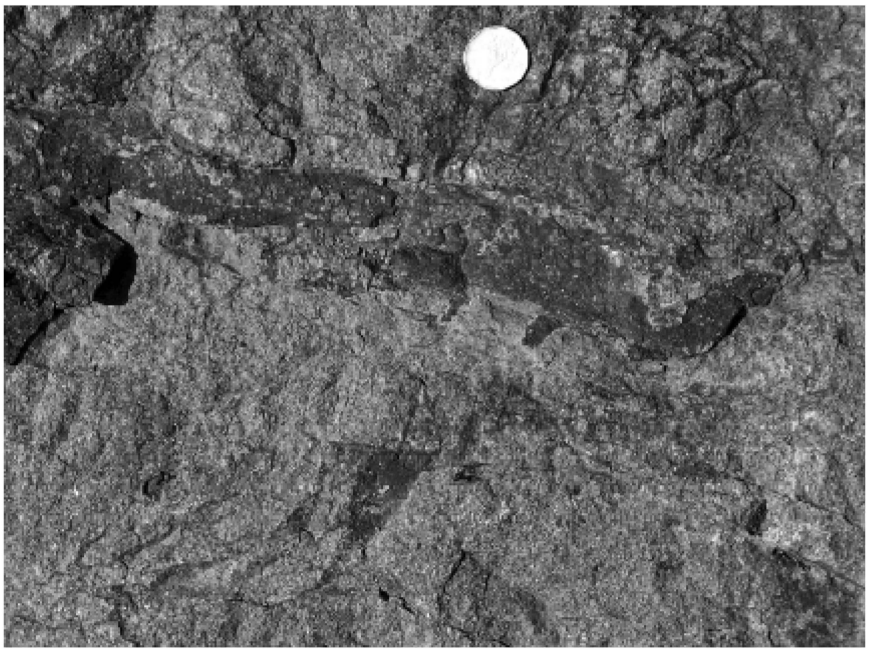

Fig. 6. A cataclasite vein with apophyses and lithic clasts occurs within the monomict breccia ring. This breccia vein lacks a melt matrix. The clasts are angular to sub-angular and varied in size. The diameter of the coin is 2.5 cm.

± biotite, zircon, apatite, magnetite, sphene, with small amounts of chlorite, calcite, epidote, and sericite, is foliated in places, and moderately altered (plagioclase to sericite; hornblende to chlorite). The quartz from GQV is mostly milky white in color, crystalline, contains sericite, is dusted with opaques, exhibits undulose extinction, and locally shows dynamic recrystallization in the form of subgrain development. The dolerites are dark greenish-grey in color, fine- to medium-grained, altered, and extensively brecciated in the Dhala area. They comprise hornblende (retrograde after clinopyroxene), chlorite, sericite (after plagioclase), epidote, and opaques.

Two distinct breccia types are observed in parts of the Dhala area. The first breccia type consists of extensively fractured and partially brecciated granitoids that also contain some xenoliths (ironstone and calc-silicate rocks, felsic volcanics, vein quartz, and dolerite components). The granitoids constitute the by far dominant clast population; clast sizes range up to a meter, and clast:matrix ratios vary between 95:5 and 60:40. The matrix (defined as the optically not resolvable material) is pink/purple colored, overall fine-grained and ferruginous, and contains quartz, opaque minerals, mica, and rock fragments. The clast population of this breccia is dominated by granitoids (>95%) besides small amounts derived from the various xenolith components.

The rock type can be defined as a monomict breccia with clastic matrix (as determined by optical microscopy) containing lithic and mineral clasts that locally carry thin (0.2 to 5 cm) cataclasite veins (Fig. 6). The finest-grained material is optically unresolved but appears as a mixture of phyllosilicate alteration and felsic mineral particles. These dark, purplish-brown colored, very fine-grained, matrix-bearing (clast to matrix ratio of 65:35) vein samples comprise angular to subangular clasts of lithic fragments (up to 2 cm in size), quartz (up to 5 mm), feldspar (up to 1 mm), and other minor phases (chlorite, zircon, opaque, and apatite). No evidence of possible melt components has been detected in these breccias.

The second breccia type is of reddish/orange color, aphanitic to fine-grained crystalline, contains lithic and mineral clasts (clast:matrix ratios range from 80:20 to 60:40) set in a devitrified groundmass, exhibits flow structures locally in both the matrix and in selected clasts (Figs. 7a and 7b), and is, in part, highly vesicular. Numerous ovoid or droplet-shaped to pipe-like vesicles occur, most with a filling of either calcite, quartz, chlorite, smectite, or agate of <1 mm to 6 cm sizes. The quartz fillings are fresh in appearance, in contrast to the toasted and generally dusted looking, primary quartz clasts. The lithic clasts range in size from 1 mm to 20 cm. The clast content in this melt breccia is variable and ranges from <10 to >40 vol%. The fine-grained groundmass is composed mainly of feldspar spherulitic and garben-shaped (Fig. 7c) devitrification products set in a submicroscopic matrix. Also skeletal (hollow, H-shaped, and swallow-tail) plagioclase microlites are frequently observed. Lighter areas of matrix also display abundant garben or spherulitic aggregates of whisker crystallites of what is thought to be phyllosilicate (products of alteration possibly after pyroxene or amphibole). The dark color of the matrix is due to the presence of extremely fine-grained opaque minerals (probably magnetite or ilmenite) and some pyroxene or amphibole crystals throughout the groundmass. Major clast types are sub-angular

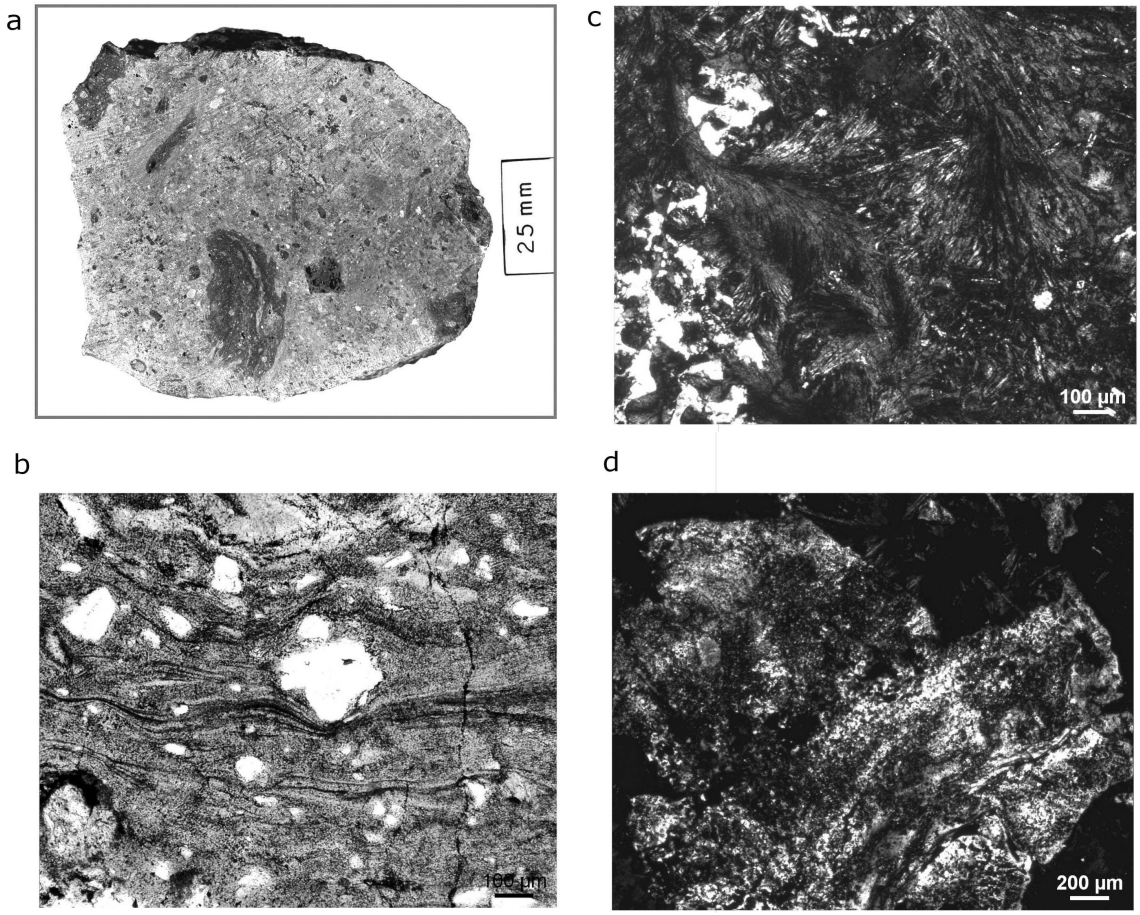

Fig. 7. a) A slice of a melt breccia sample showing lithic (mostly granitoid) and mineral clasts in an aphanitic matrix. The clasts are of varied size. Flow structure is visible in a dark lithic clast. b) Compositionally (felsic versus mafic) as well as flow banded melt rock. The very light-colored streaks are essentially silica. Note the flow features around some larger clasts (plane polarized light). c) Finest-grained crystalline impact melt rock showing radial and garben shaped assemblages of plagioclase crystallites. Note the partially recrystallized nature of the relatively rare clasts (crossed polarizers). d) "Chert-like" recrystallization of quartz clasts in aphanitic, locally devitrified (upper right—skeletal plagioclase crystals) groundmass of a melt breccia sample (crossed polarizers).

to sub-rounded in shape, partly digested, and show random orientation. Flow lines in the melt breccia also show varied orientations. Some of the quartz clasts enclose a devitrified melt phase. Minor phases in the matrix include euhedral zircon, chlorite, dusty-appearing opaque minerals, and apatite. Nearly the entire clast content seems to be derived from granitoid precursors, with a few metasedimentary (meta-ironstone) or calc-silicate clasts likely derived from xenoliths in the granitoid country rocks. Some of the clasts have elongated forms possibly suggestive of plastic deformation. Many quartz clasts are completely recrystallized to very fine-grained, chert-like material (Fig. 7d). Presumably these grains represent annealed silica melt (after diaplectic glass or lechatelierite). The main alteration phase in the melt breccia and that is responsible for the dark reddish color of the breccia is very fine-grained and comprises disseminated Fe-oxide/hydroxide (likely goethite). The lighter reddish matrix also contains a significant amount of secondary phyllosilicates.

The post-Dhala rocks include sediments of pre-Vindhyan age and of the Semri Group of the Vindhyan Supergroup, which have been dated at 1.601 ± 0.13 Ga (Ray et al. 2003). The pre-Vindhyan sedimentary rocks are exposed mostly in water well sections that show alternating sandy siltstone and siltstone with local conglomerate horizons that pinch out laterally. These rocks are massive to well laminated and have subparallel to wavy stratification. The sandy siltstones are green-white in color and comprise subangular to subrounded quartz (up to a mm in size) with small amounts of mica, opaques, zircon and tourmaline in a clay-rich matrix (clast: matrix = 70:30 by volume). The tourmaline grains are mostly rounded and zircon grains are rounded to subrounded. The siltstone is purplish brown in color and contains quartz clasts in a ferruginous clay-rich matrix. The quartz grains are subangular to subrounded in shape, measure less than a mm in size, and are well sorted. They commonly are zoned with distinct overgrowth zones. The lenticular pockets of conglomerates are clast-supported, polymict (chert, jasper, and quartz), and moderately sorted.

The sediments belonging to the Vindhyan Supergroup are

exposed in the central elevated area. They include a repetitive succession of greenish-yellow shale and arenite with locally occurring, thin, intercalated beds of pebbly sandstone-conglomerate. The shale comprises quartz grains with undulose extinction, abundant biotite and chlorite, with a few kinked biotite grains, and opaque phases in a clay-rich matrix.

PETROGRAPHIC EVIDENCE FOR AN IMPACT ORIGIN OF THE DHALA STRUCTURE

One hundred and thirteen thin sections of the various rock types from 12 localities in the Dhala structure were studied by optical microscopy (sample locations are shown in Fig. 3). The presence of diagnostic shock metamorphic features was only noted in samples of melt breccia. Quartz and feldspar mineral and lithic granitic clasts in melt breccia contain diagnostic shock metamorphic features, such as multiple sets of planar deformation features (up to 5 sets of PDFs per grain; Figs. 8a and 8b) in quartz and feldspar, ballen-textured quartz (Figs. 8c–e) after diaplectic glass or lechatelierite (e.g., Stöffler and Langenhorst 1994), and checkerboard feldspar (Fig. 8f). The percentage of shocked quartz and feldspar grains in the impact melt breccia is variable (7 to 67% of the quartz grains studied in a given thin section). It is estimated that 30% of the 2500 quartz grains studied contain PDFs. The number of PDFs observed in different quartz and feldspar clasts within one sample is highly variable. Most PDFs are of the decorated type; many shocked quartz grains appear toasted (Short and Gold 1996; Whitehead et al. 2002). The width of PDFs ranges from less than 1 to about 3 μm. The spacings of the PDFs range from 2 to 8 μm. Fluid inclusions are ubiquitous along the PDF. Most PDFs are observed across the entire width of the host grain, but in ballen-bearing quartz PDFs may also occur as remnants within individual ballen.

Ballen quartz is very common in nearly all the samples of impact melt breccia studied so far. There are two types of ballen quartz in Dhala melt breccia samples—with continuous extinction of ballen and with discontinuous optical extinction (compare discussion in Grieve et al. [1996] and Ferierre et al. [Forthcoming]). Size, shape, and number of ballen vary within individual quartz grains and from one grain to another (Pati et al. 2006). Four thin sections of melt breccia containing 31 quartz grains with 448 individual ballen were evaluated with regard to ballen diameter. The average diameter observed is 49 ± 11 μm; the maximum and minimum values are 163 and 12 μm, respectively. The ballen rim thickness varies from 1.6 to 6.3 μm. Ballen show varied shape, size, and distribution density from grain to grain, within a given thin section. A number of domains with varied sizes and shapes of ballen in a single grain are also observed. In some ballen-bearing quartz, larger ballen are observed in the center of the grain compared to the peripheral area, whereas the opposite is observed in others. The host grain size is not directly proportional to the particular population of ballen loops in terms of ballen size and distribution. It is also observed that the ballen loops may or may not show "toasting," with brownish solid and fluid inclusions. In some cases, remnant PDFs are found within ballen quartz grains (Fig. 8e).

Checkerboard-textured feldspar (Fig. 8f) occurs commonly in the melt breccia and consists of 5–50 μm sized clear subgrains of variable optical orientation in an aphanitic matrix and is found in feldspar-bearing granitoid clasts within melt breccia. Plagioclase occurs both as sub-angular feldspar clasts as well as skeletal grains in the melt matrix. A checkerboard feldspar grain showed the development of a reaction rim suggesting chemical reaction with the melt phase.

Fluidal-textured, obviously plasticized clasts (Fig. 8g) are abundant in impact melt breccia samples. The schlieren in melt breccia matrix vary in color from light yellowish to brown to dark brownish or gray, and they locally contain abundant microlites of feldspar and possibly pyroxene, as well as an as yet unidentified oxide mineral (likely ilmenite or magnetite). Other clast types in melt breccia include quartzite (possibly from calc-silicate rock), fine-grained ferruginous clasts with quartz grains, and aphanitic melt clasts with perlitic cracks (Fig. 9). The study of these other clast types so far did not reveal the presence of any diagnostic shock metamorphic features, although planar fractures and kink-banded micas are observed, and the dissociation of mafic minerals to oxides was noted. Samples collected along the extent of impact melt breccia exposures did not reveal any systematic change in terms of clast population or proportion of shock metamorphosed clasts. A single quartz clast (Fig. 10) was observed that contains a small cluster of tiny coesite crystals, the presence of which was confirmed by Raman spectroscopy. Zircons in melt breccia are invariably zoned, appear turbid, rarely contain planar fractures or granular texture (Fig. 11), show reduced birefringence, and yield the prominent Raman band at 1000.3 cm^{-1}.

FIRST GEOCHEMICAL RESULTS

Twelve samples from surface exposures and water well sections from different parts of the Dhala structure (sample locations are given in Fig. 3) were analyzed for their chemical compositions (Table 1). The samples collected for chemical characterization include six granitoid clast fragments (M-6, M-7, M-13, M-32, M-4, and M-20) from the monomict breccia ring, one sample from a granitic cataclasite vein in the monomict breccia ring (SK-2), and five samples of impact melt breccia (M-31, M-31A, SM-6, VF-04, and SK-13). Care was taken to sample fresh material without visible effects of alteration. Some of the clasts in the breccias are, however, altered to varied extent, as known from optical microscopy. Bulk samples were prepared by preselection of sample material that optically appeared clast-poor, followed by coarse-crushing and separation by handpicking of visible clasts. Major and trace element (Rb, Sr, Y, Zr, Nb, Co, Ni, Cu, Zn, V, Cr, and Ba) contents were measured by conventional

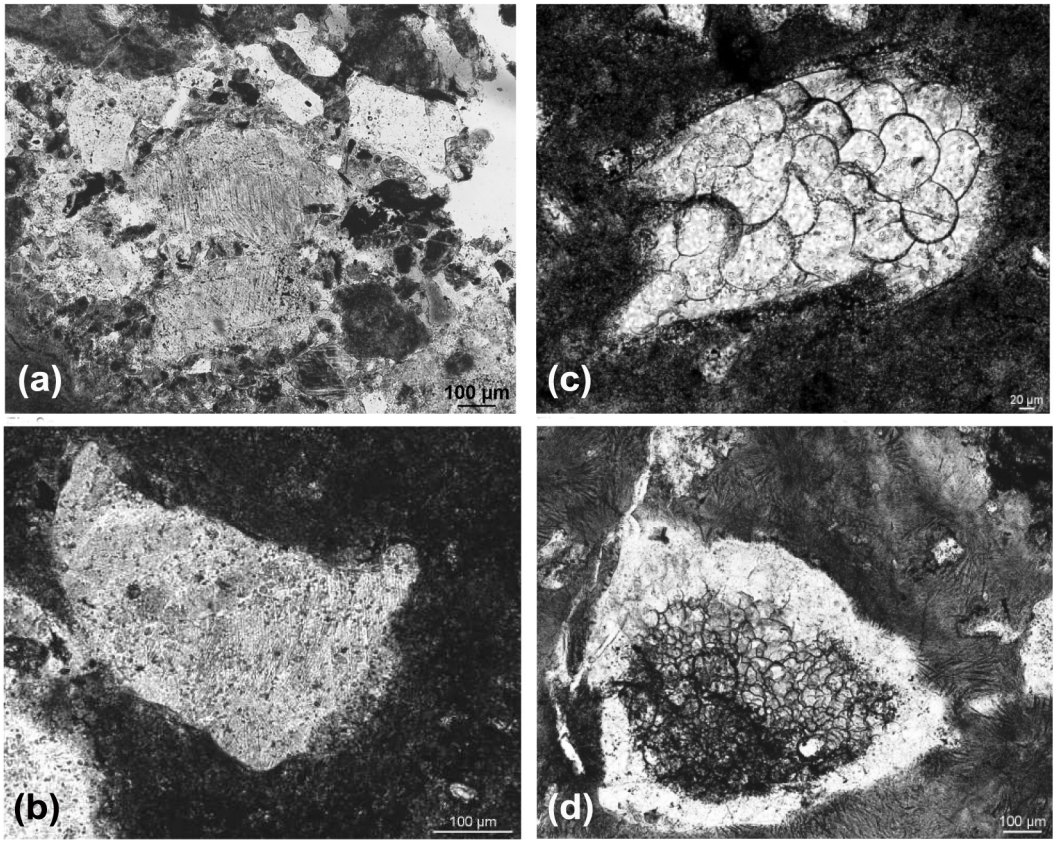

Fig. 8. Microphotographs showing different shock metamorphic features observed in Dhala impact melt breccia (all photographs taken in plane polarized light). a) Shocked quartz (toasted) grains with multiple sets of PDFs and clouded feldspar grains in the impact melt breccia. b) Largely melted shocked quartz with 4 sets of PDFs within a devitrified melt matrix. c) Largely melted quartz clast containing characteristic ballen texture showing some clear domains. d) Ballen-textured quartz showing an inner toasted and an outer clear domain in a clast set in aphanitic matrix with spherulites.

XRF methodology at the Department of Geology, University of Witwatersrand, South Africa. Abundances of other trace elements (Sc, Ni, Co, Cr, Zn, As, Se, Br, Rb, Sr, Zr, Sb, Cs, Ba, Hf, Ta, W, Ir, Au, Th, and U) and the REEs (La, Ce, Nd, Sm, Eu, Gd, Tb, Tm, Yb, Lu, Hf, and Ta) were determined by instrumental neutron activation analysis (INAA) at the University of Vienna, Vienna. Details on the analytical methods, and precision and accuracy for these XRF and INA analyses are given by Reimold et al. (1994) and Koeberl (1993), respectively.

The loss on ignition (LOI) for these samples lies between 0.37 and 3.14 ($\bar{x}$ = 1.38, n = 12) wt%, in accordance with the variable amount of secondary alteration product revealed optically. The average LOI for impact melt breccia is less ($\bar{x}$ = 1.21 wt%, n = 5) than that for granitoid breccia ($\bar{x}$ = 1.69 wt%, n = 6) and the cataclasite vein sample (1.96 wt%). The Dhala samples contain SiO_2 at 67.25 to 79.14 wt% ($\bar{x}$ = 72.71 wt%), which is significantly more than the upper crustal average of 66.0 wt% (Taylor and McClennan 1985) but close to the average Archean grey gneisses (69.8 wt%; Martin 1994). However, the average Al_2O_3 content of the Dhala samples ($\bar{x}$ =12.44 wt%) is less than that of the Archean grey gneisses (15.6 wt%; Martin 1994). It is interesting to note that the average Na_2O ($\bar{x}$ = 2.06 wt%) and K_2O ($\bar{x}$ = 6.62 wt%) contents of Dhala samples do not match the values obtained for the average for Archean grey gneisses (4.9 and 1.8 wt%, respectively; Martin 1994). The K_2O content in impact melt breccia samples is higher (8.65 wt%) than that of granitoid breccia (5.23 wt%), which is attributed to post-impact alteration of impact melt breccia, similar to the observation of French et al. (1997) and the work referenced therein for a number of other impact structures worldwide.

Most major element data for Dhala samples show scatter when compared with respective SiO_2 contents, except for TiO_2, Al_2O_3, and CaO, where very slight negative correlation is observed. The K_2O content shows a negative correlation with the SiO_2 content in case of impact melt breccia but a positive correlation is noted for the granitoid breccia analyses. The reverse is true for the Na_2O versus SiO_2 contents for the same samples. The Na_2O/K_2O ratio of impact melt breccia is very low (0.13) compared to the ratios for granitoid breccia (0.52) and cataclasite (0.57). Similar variations in alkali metal ratio between the impact melt breccia and target rocks have been noted in other impact

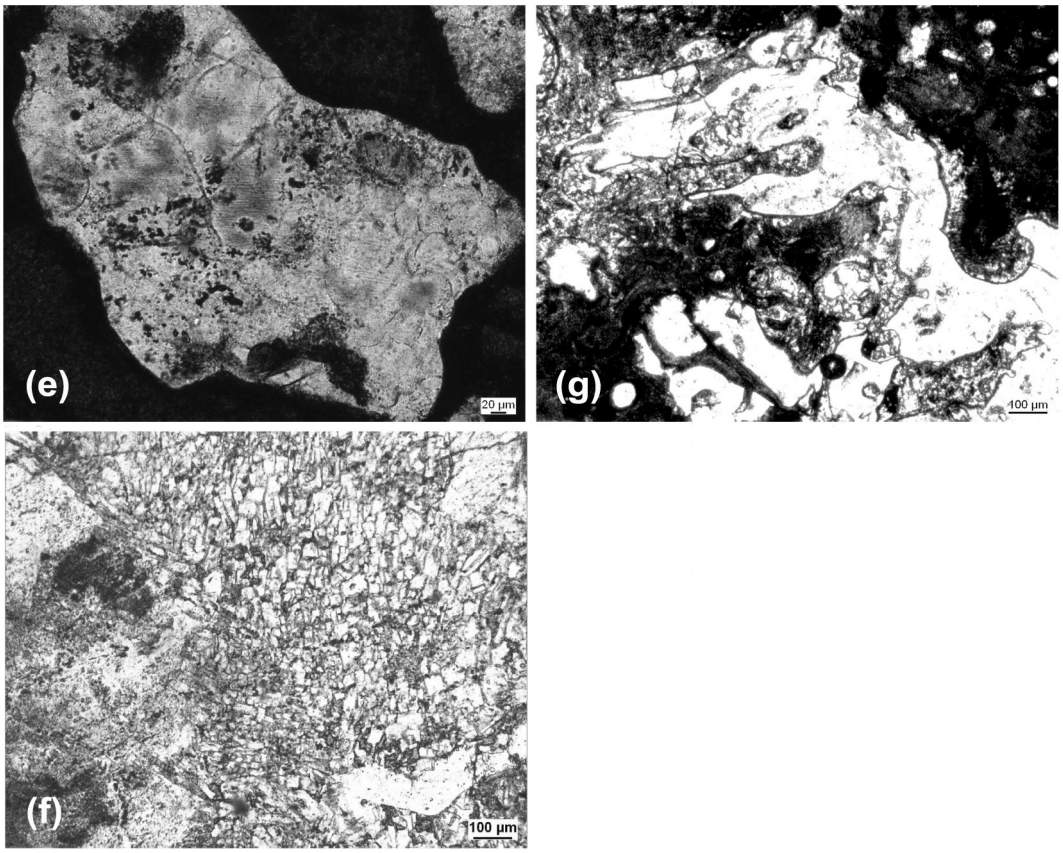

Fig. 8. *Continued*. Microphotographs showing different shock metamorphic features observed in Dhala impact melt breccia (all photographs taken in plane polarized light). e) Ballen quartz with remnant sets of PDF. Note the distinct ballen rims especially in the right part of the image. f) Checkerboard feldspar is observed within a granitoid clast occurring in impact melt breccia with anhedral quartz and clouded feldspar grains. g) Fluidally stretched shock melted quartz in devitrified melt matrix.

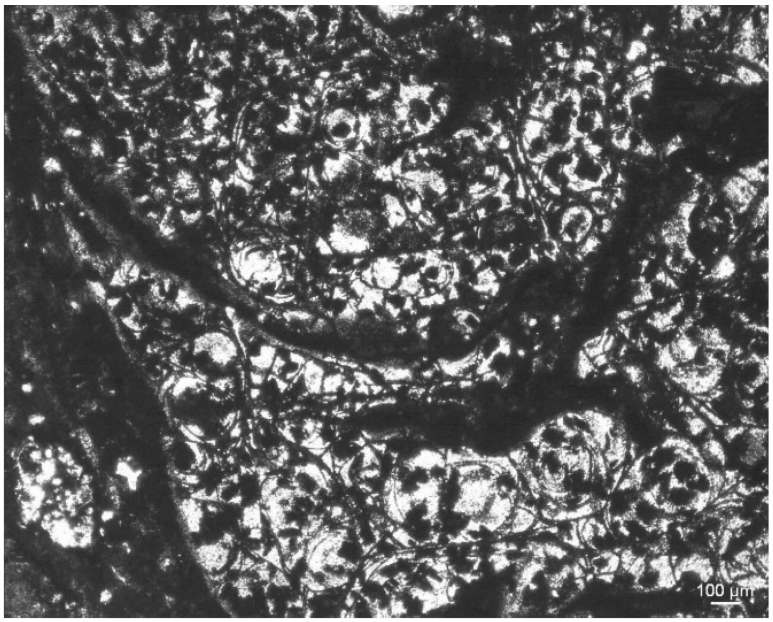

Fig. 9. Evidence for complete rock melting is seen under plane polarized light in the form of an aphanitic grain showing perlitic devitrification texture comprising circular cracks and growth of dark-colored crystallites.

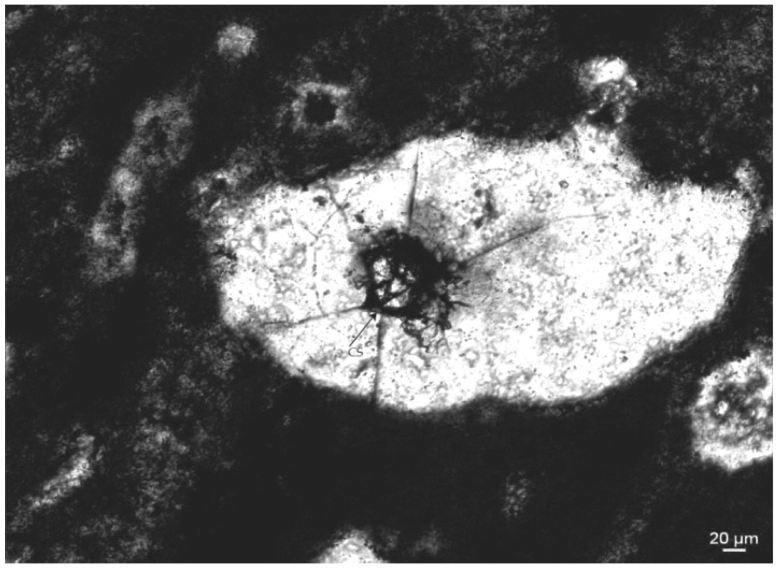

Fig. 10. A ballen-textured and PDF-bearing quartz grain from Dhala impact melt breccia shows characteristic radial cracks emanating from an aggregate of coesite grains in the center of the image (plane polarized light).

structures also (e.g., Koeberl et al. 2001) and frequently attributed to hydrothermal alteration. The abundances of the trace elements Cr, Co, Ni and Sc in the Dhala samples are highly variable. The values for Cr, Co, and Ni are close to upper crustal average (85, 17, and 44 ppm, respectively; cf. Taylor and McLennan 1985) or slightly below it. However, the Ni content in impact melt breccia samples (38 ppm) is significantly higher than that of granitoid breccia samples (19 ppm). The limited number of samples analyzed for Ir abundances does not indicate the presence of a meteoritic component in the impact melt breccia, as Ir values are close to or below the detection limit (1.0 ppb) for the INAA data. Where Ir concentrations could be determined (Table 1), the melt rock breccia contains 0.8 ppb Ir compared to 0.1 ppb in the target granitoids. However, because of the proximity to the detection limit, these data are most likely not reliable. For these breccias, the Ir values show positive correlation with Cr and Ni contents.

The contents of Ba, Rb, and Cs do not show any correlation with respect to K_2O contents, suggesting that these elements are not solely concentrated in K-feldspar. Similarly, a Zr-SiO_2 plot reflects a negative trend, although most of these samples show abundant zircon. The positive correlation of the contents of Zr and Hf and the average Zr/Hf ratio of 40.7 (zircon has a value of 39; Murali et al. 1983) support the petrographic recognition of zircon. The concentrations of Th and U in the impact melt breccia (26.5 and 3.93 ppm, respectively) are higher than the average values for the granitoid breccia samples (23.3 and 3.50 ppm, respectively) and the cataclasite (15.9 and 4.25 ppm, respectively). The average Th/U ratio of 7.77 for all these samples is higher than the upper continental crust average of 3.8 (Taylor and McLennan 1985), suggesting the possible oxidation and leaching of uranium, and is in keeping with the regional investigation of possible uranium mineralization by government agencies.

The chondrite-normalized (after Taylor and McLennan 1985) rare earth element (REE) abundance patterns (Fig. 12) indicate that the impact melt breccia, the granitoid breccia, and the cataclasite sample show nearly similar patterns with enriched light rare earth elements (LREE), depleted heavy rare earth elements (HREE), and a negative Eu anomaly ($Eu/Eu^* < 1$). Most samples have a slight negative Eu anomaly (Eu/Eu^*= 0.50–0.83) with an average Eu/Eu^* of 0.65. The impact melt breccia and granitoid breccia have similar Eu/Eu^* values of about 0.7. The LREE depletion in impact melt breccia is directly proportional to the SiO_2 content in the bulk rock and inversely proportional to the K_2O concentration. Thus, the large variation in LREE content in these samples is controlled by the abundance of K-feldspar, which is also reflected in the normative orthoclase content (64.5 to 31.5%). The LREE enrichment and HREE depletion, with a variable negative Eu anomaly, observed here is typical of Bundelkhand granitoids (Pati et al. 2007). Slight variability in normalized LREE abundance within the analyzed sample set could be due to varied proportions of quartz and feldspar clasts in the respective samples or by the preferential dissolution of K-feldspar in the melt phase. The La_N/Yb_N ratio varies between 2 and 20.6, suggesting a non-uniform fractionation pattern.

THE AGE OF THE DHALA STRUCTURE

The absolute age of the Dhala impact event is not yet known. The radiometric ages of the target rocks and the cover sediments from the Dhala area, in particular, have not been

Table 1. Chemical composition of melt breccia, granitoid clasts and a granitic cataclasite vein sample from the Dhala structure (major element data in wt%; all Fe as Fe_2O_3; trace element data in ppm unless stated otherwise).

Sample no.	M-31 melt breccia	M-31A melt breccia	SM-6 melt breccia	VF-04 melt breccia	SK-13 melt breccia	M-6 granitoid breccia	M-7 granitoid breccia	M-13 granitoid breccia	M-32 granitoid breccia	M-4 granitoid breccia	M-20 granitoid breccia	SK-2 cata-clasite
SiO_2	77.65	71.23	77.64	69.73	70.19	73.58	70.59	79.14	73.82	67.25	71.54	70.14
TiO_2	0.29	0.36	0.09	0.32	0.35	0.27	0.33	0.04	0.15	0.41	0.41	0.32
Al_2O_3	9.74	11.94	11.29	14.78	14.05	12.61	14.75	10.52	11.18	13.49	12.57	12.33
Fe_2O_3	2.48	5.35	0.97	1.70	2.13	1.79	3.45	1.18	2.05	5.63	4.26	4.96
MnO	0.02	0.03	0.02	0.03	0.03	0.03	0.06	0.01	0.10	0.05	0.08	0.05
MgO	0.11	0.00	0.00	0.05	0.87	0.47	0.51	0.00	0.23	3.41	2.19	1.54
CaO	0.26	0.20	0.21	0.27	0.48	0.32	0.74	0.04	1.23	0.31	0.42	0.34
Na_2O	1.20	0.29	3.70	0.30	0.24	0.91	3.12	2.85	4.31	2.97	2.07	2.74
K_2O	6.94	9.78	5.28	10.96	10.29	9.14	5.04	5.33	4.59	3.82	3.47	4.81
P_2O_5	0.07	0.09	0.00	0.03	0.05	0.05	0.09	0.00	0.02	0.10	0.12	0.10
LOI	0.83	0.43	0.42	1.32	1.52	0.92	1.60	0.37	1.31	2.79	3.14	1.96
Total	99.59	99.70	99.62	99.49	100.20	100.09	100.28	99.48	98.99	100.23	100.27	99.29
Sc	3.08	4.75	1.04	3.99	4.13	3.61	4.48	0.54	2.83	7.47	8.98	6.35
Cr	33.2	66.6	6.44	17.6	20.5	4.22	8.31	8.01	7.50	43.1	110	39.4
Co	2.86	4.77	0.82	2.70	3.86	1.54	4.32	0.98	3.18	10.4	14.3	11.0
Ni	34	60	8	35	5	5	13	4	23	21	47	31
Zn	11	15	5	16	28	40	35	6	14	86	113	67
As	4.91	3.51	1.34	1.14	<1.76	1.83	1.35	1.01	8.42	1.84	0.67	5.86
Se	0.2	0.05	0.15	0.1	<0.2	<0.2	0.1	<0.1	0.06	<0.3	0.4	<0.3
Br	0.5	0.5	0.7	0.8	0.7	0.7	0.8	0.5	0.6	0.8	0.3	0.7
Rb	163	192	214	213	220	285	213	254	213	118	105	171
Sr	38	42	86	48	25	88	137	36	36	78	87	84
Zr	135	225	115	263	239	198	226	62	287	169	220	198
Ru	6.66	9.30	7.50	15.6	10.1	31.6	13.6	2.68	4.11	11.3	12.7	9.78
Sb	0.64	1.07	0.19	0.43	0.27	0.07	0.22	0.12	0.31	0.45	0.22	0.46
Cs	0.70	0.66	2.89	1.74	3.60	0.16	6.95	2.32	2.01	1.19	0.55	1.46
Ba	497	786	508	1036	676	1999	988	170	385	753	886	684
La	22.5	54.9	6.29	67.1	52.8	92.2	56.7	5.41	39.2	50.2	46.5	63.2
Ce	39.4	97.2	11.7	121	91.0	161	91.0	11.1	75.0	90.6	97.0	113
Nd	13.8	35.0	4.69	41.3	33.1	62.9	29.8	4.63	33.1	37.4	37.4	44.2
Sm	2.55	5.84	0.99	6.81	5.51	9.40	4.51	1.26	7.92	6.42	6.88	7.24
Eu	0.53	1.06	0.27	1.50	1.16	0.51	0.91	0.29	1.93	1.21	1.69	1.47
Gd	2.35	3.59	1.83	4.48	4.66	<0.95	3.15	2.5	8.11	3.59	7.09	4.19
Tb	0.36	0.73	0.31	0.74	0.78	0.60	0.48	0.40	1.62	0.61	0.97	0.73
Tm	0.18	0.38	0.31	0.38	0.28	<0.02	0.31	0.30	0.64	0.33	0.48	0.39
Yb	1.18	2.19	2.18	2.41	2.16	3.27	1.86	1.61	4.78	1.76	2.67	2.11
Lu	0.19	0.36	0.37	0.40	0.34	0.51	0.31	0.25	0.73	0.26	0.42	0.31
Hf	3.10	4.36	6.93	5.18	4.95	8.56	5.43	2.41	11.2	3.70	3.93	3.35
Ta	1.27	1.64	3.01	2.25	2.08	1.06	3.60	1.08	7.86	1.31	2.27	1.77
Ir (ppb)	<0.8	0.8	0.1	<0.7	0.4	<1.5	<0.4	<0.5	<2	<1	<0.6	<1
Au (ppb)	<1	0.3	0.3	0.4	0.4	<1.2	0.5	<0.8	0.7	2.6	<1.8	<1.6
Th	19.4	24.3	22.5	34.6	31.7	22.6	29.5	23.9	34.9	17.5	10.7	15.9
U	2.46	4.87	2.71	4.94	4.69	4.72	1.64	1.71	7.58	4.18	1.19	4.25
K/U	23,491	16,747	16,229	18,486	18,286	16,144	25,682	25,967	5049	7619	24,395	9425
La/Th	1.17	2.26	0.28	1.94	1.67	4.08	1.92	0.23	1.12	2.88	4.32	3.98
Th/U	7.86	5.00	8.30	7.00	6.75	4.78	18.03	13.98	4.61	4.18	9.07	3.74
Zr/Hf	43.6	51.6	16.5	50.8	48.3	23.2	41.7	25.8	25.6	45.7	55.9	59.3
La_N/Yb_N	12.9	16.9	2.0	18.8	16.5	19.0	20.6	2.27	5.55	19.3	11.8	20.3
Eu/Eu^*	0.66	0.71	0.61	0.83	0.70	–	0.74	0.50	0.74	0.77	0.74	0.82

determined. The oldest meta-supracrustal rocks of TTG affinity from the Bundelkhand craton are known to be of 3.5 (Sarkar et al. 1996) to 3.3 Ga (Mondal et al. 2002) age, based on Rb-Sr isochron work and $^{207}Pb/^{206}Pb$ single-crystal zircon dating, respectively. The geochronological data for various felsic intrusives constrain their emplacement ages between 2.2 and 2.5 Ga (Sarkar et al. 1996; Mondal et al. 2002). Pb-Pb dating by ion microprobe analysis of the gneissic rocks exposed in the Karera area (~15 km north of Dhala) and of a hornblende-granitoid from the Jakhaura area (~50 km southwest of the Dhala structure) yielded ages of 2563 ± 6 and 2516 ± 4 Ma, respectively (Mondal et al. 2002). The mafic dike swarms in parts of the Bundelkhand craton were dated by the $^{40}Ar/^{39}Ar$ stepheating method and revealed two

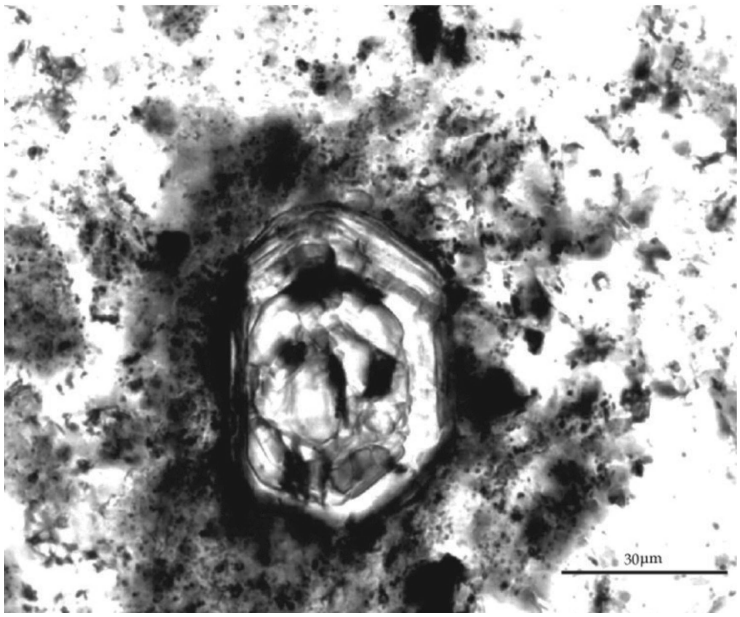

Fig. 11. Nearly colorless, subhedral shocked zircon grain with granular texture in some parts and multiple zonation in others; from an impact melt breccia sample (plane polarized light).

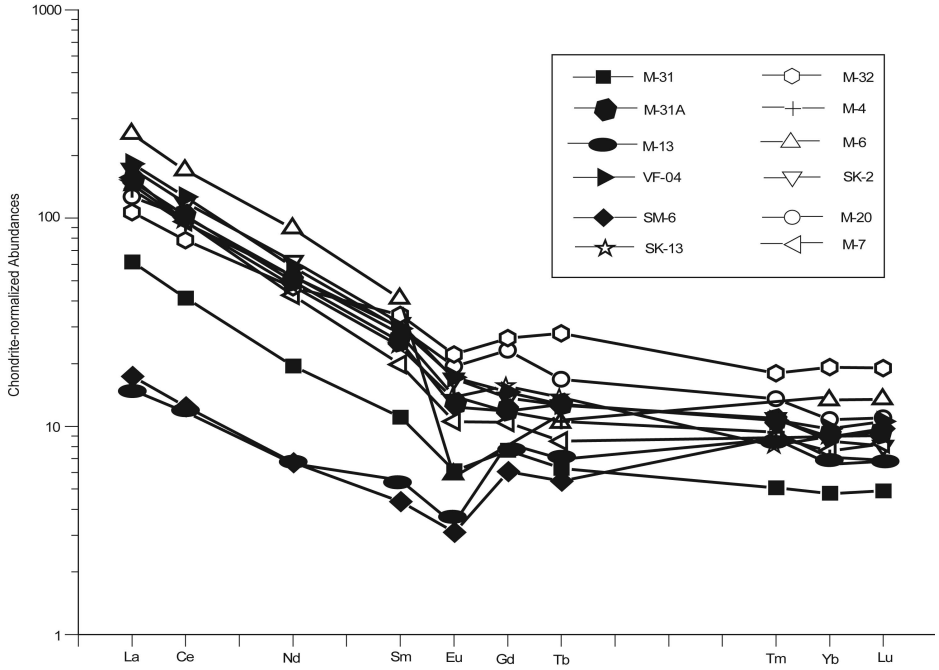

Fig. 12. Chondrite-normalized REE patterns of impact melt breccia, granitoid breccia from the monomict breccia ring, and a granitic cataclasite. The normalization values are after Taylor and McLennan (1985). The solid symbols denote the impact melt breccia samples and the open symbols are for the granitoid breccia samples and a granitic cataclasite.

episodes of magmatism at 2000 and 2150 Ma, respectively (Rao et al. 2005). The argillaceous-arenaceous sediments belonging to the Semri Group (Jain et al. 2001) overlie the Bundelkhand granitoids with an unconformable contact in the Dhala area.

The Archean and Paleoproterozoic basement is covered widely by strata of the Vindhyan Supergroup, occurring in parts of the Central Indian Shield with a maximum thickness of about 4500 m (Ahmad 1958; Chakraborty and Bhattacharyya 1996). The Vindhyan Supergroup was deposited after the stabilization of the Aravalli-Bundelkhand (also known as Bhandara) craton around the time of completion of felsic magmatism at about 2.2 Ga (Chakraborty 2006). These sediments are unmetamorphosed and nearly

undeformed (Ray 2006). The Vindhyan Supergroup has been subdivided into Lower (Semri Formation) and Upper sequences (Kaimur, Rewa, and Bhander Formations) (Banerjee et al. 2006; Chakraborty 2006). In general, the Semri Group (or pre-Kaimur Formation) comprises mostly marine sediments that include carbonates, siliciclastics, and volcaniclastics (Banerjee et al. 2006). The age of the Lower Vindhyan rocks (silicified tuffs bounding the Chorhat Sandstone, Semri Group) as determined by SHRIMP U-Pb zircon chronology is bracketed between >1700 Ma and 1601 ± 130 Ma (Ray et al. 2003). The oldest age of a Vindhyan Supergroup component reported so far is 1721 ± 90 Ma (Pb-Pb isochron method; Sarangi et al. 2004; Kajrahat limestone, Son valley).

The mafic dikes (2000–2150 Ma; Rao et al. 2005) represent the youngest pre-impact rock type in the Dhala area and the age of the post-impact cover sediments is considered to be about ~1700 Ma. Hence, the age of the Dhala impact event can be constrained between about 2100 and 1700 Ma.

Recently, first SHRIMP U-Pb single-zircon and argon step heating attempts to date impact melt breccia from Dhala were made by our group (Jourdan et al. 2008), but failed to better constrain the age of the impact event. Zircon chronology yielded ages typical for the regional basement granitoids, and the argon dating results relate to post-impact overprint (~1–0.8 Ga). The full results will be published elsewhere. It has, however, become clear that it will only be possible to further constrain the age of the Dhala impact structure when less altered impact melt rock will become available.

SUMMARY AND CONCLUSIONS

The Dhala structure formed in Archean crystalline basement of the Bundelkhand craton in the Central Indian Shield was previously called the "Mohar Cauldron" by Jain et al. (2001), Srivastava et al. (2002), and Srivastava and Nambiar (2003). The presence of shock metamorphic features, such as PDFs, ballen-textured quartz, coesite, and checkerboard feldspar in melt breccia confirms the impact origin of the Dhala structure. Isolated outcrops of impact melt breccia could represent remnants of an originally much wider sheet complex of impact melt breccia. The possibility is entertained that these patchy outcrops are connected below surface, and possibly forms (or formed) a sheet-like layer above the monomict breccia of the interior of the structure. The Dhala impact structure has an apparent minimum diameter of about 11 km, as indicated by the currently accessible exposures of monomict impact breccia. As a large part of the area is covered by alluvium, the present measured diameter possibly represents a minimum estimate. The structure represents the eroded remnant of the largest impact structure currently known from the Indian subcontinent, and in fact from the wider region between the Middle East and southeastern Asia. Preliminary geochemical analysis showed that impact melt rock and granitic basement have similar compositions, in accordance with the petrographic finding that granitoid clastic material forms the overwhelming proportion of the clast content of the melt breccia. Thus, it is unlikely that a major supracrustal component of the target region has not been sampled by us. No meteoritic component has so far been detected in the melt breccia, but further geochemical work is in progress.

The age of the Dhala structure is so far only loosely constrained by the ages of the impacted basement (mafic dykes) of >2.1 Ga and of the overlying supracrustals of the Vindhyan Supergroup at <1.6 Ga.

Acknowledgments—J. K. P. thanks the Department of Science and Technology, New Delhi for providing a research microscope through a grant (no. ESS/16/195/2003) and the PLANEX program of the Department of Space, Government of India, and for funding this present study. Sharon Turner at the University of the Witwatersrand kindly supported us with XRF analysis. Analytical work in Vienna was supported by the Austrian Science Foundation (grant P18862-N10 to C. K.). Detailed reviews by Wright Horton Jr. and Gordon Osinski are much appreciated.

REFERENCES

Ahmad K. 1958. Paleogeography of Central India in the Vindhyan period. *Geological Survey of India Records* 87:531–548.

Banerjee S., Dutta S., Paikaray S., and Mann U. 2006. Stratigraphy, sedimentology and bulk organic geochemistry of black shales from Proterozoic Vindhyan Supergroup (central India). *Journal of Earth System Science* 115:37–47.

Basu A. K. 1986. Geology of Bundelkhand granite massif, Central India. *Geological Survey of India Records* 101:61–124.

Basu A. K. 2004. Contemplations on the role of the Bundelkhand massif on structural evolution and mineralization in the Western Indian craton, Rajasthan, India. *Geological Survey of India Special Publication* 72:325–344.

Chakraborty C. 2006. Proterozoic intracontinental basin: The Vindhyan example. *Journal of Earth System Science* 115:3–22.

Chakraborty C. and Bhattacharyya A. 1996. The Vindhyan basin: An overview in the light of current perspectives. In *Recent advances in Vindhyan geology*, edited by Bhattacharyya A. *Memoir Geological Society of India* 36:301–312.

Chatterjee S., Guven N., Yoshinobu A., and Donofrio R. 2006. Shiva structure: A possible KT boundary impact crater on the western shelf of India. Texas Technical University Natural Science Research Laboratory Special Publication #50. 39 p.

Earth Impact Database. 2008. www.unb.ca/passc/Impact/Database. Last accessed 15 February 2008.

Ferriere L., Koeberl C., and Reimold W. U. Forthcoming. Characterisation of ballen quartz and cristobalite in impact breccias: New observations and constraints on ballen formation. *European Journal of Mineralogy.*

Fredriksson K. A., Dube A., Milton D. J., and Balasundaram M. S. 1973. Lonar Lake, India: An impact crater in basalt. *Science* 180: 862–864.

French B. M. 1998. *Traces of catastrophe; A handbook of shock-metamorphic effects in terrestrial meteoritic impact structures*. LPI Contribution #954. Houston: Lunar and Planetary Institute. 120 p.

French B. M., Koeberl C., Gilmour I., Shirey S. B., Dons J. A., and

Naterstad J. 1997. The Gardnos impact structure, Norway: Petrology and geochemistry of target rocks and impactites. *Geochimica et Cosmochimica Acta* 61:873–904.

Grieve R. A. F., Langenhorst F., and Stöffler D. 1996. Shock metamorphism in nature and experiment: II. Significance in geoscience. *Meteoritics & Planetary Science* 31:6–35.

Jain S. C., Gaur V. P., Srivastava S. K., Nambiar K. V., and Saxena H. P. 2001. Recent find of a cauldron structure in Bundelkhand craton. Geological Survey of India Special Publication #64: 289–297.

Jourdan F., Reimold W. U., Armstrong R. A., Pati J. K., Renne P., and Koeberl C. 2008. Elusive age of the Paleoproterozoic Dhala impact structure, India: First SHRIMP U-Pb and argon chronological results (abstract #1244). 39th Lunar and Planetary Science Conference. CD-ROM.

Koeberl C. 1993. Instrumental neutron activation analysis of geochemical and cosmochemical samples: A fast and proven method for small sample analysis. *Journal of Radioanalytical and Nuclear Chemistry* 168:47–60.

Koeberl C., Reimold W. U., and Kelly S. P. 2001. Petrography, geochemistry, and argon-40/argon-39 ages of impact-melt rocks and breccia from the Ames impact structure, Oklahoma: The Nicor Chestnut 18-4 drill core. *Meteoritics & Planetary Science* 36:651–669.

Malviya V. P., Arima M., Pati J. K., and Kaneko Y. 2006. Petrology and geochemistry of metamorphosed basaltic pillow lava and basaltic komatiite in Mauranipur area: Subduction related volcanism in Archean Bundelkhand craton, Central India. *Journal of Mineralogical and Petrological Sciences* 101:199–217.

Martin H. 1994 Archean grey gneisses and the genesis of the continental crust. In: *Archean crustal evolution*, edited by Condie K. C. Amsterdam: Elsevier. 205 p.

Master S. and Pandit M. K. 1999. New evidence for an impact origin of Ramgarh Structure, Rajasthan, India (abstract). *Meteoritics & Planetary Science* 34:A79.

Mondal M. E. A., Goswami J. N., Deomurari, and Sharma K. K. 2002. Ion microprobe $^{207}Pb/^{206}Pb$ ages of zircons from the Bundelkhand massif, northern India: Implications for crustal evolution of the Bundelkhand-Aravalli protocontinent. *Precambrian Research* 117:85–100.

Murali A. V., Parthasarathy R., Mahadevan T. M., and Sankar Das M. 1983. Trace element characteristics, REE patterns, and partition coefficients of zircons from different geological environments—A case study on Indian zircons. *Geochimica et Cosmochimica Acta* 47:2047–2052.

Osae S., Misra S., Koeberl C., Sengupta D., and Ghosh S. 2005. Target rocks, impact glasses, and melt rocks from the Lonar impact crater, India: Petrography and geochemistry. *Meteoritics & Planetary Science* 40:1473–1492.

Pati J. K. 2005. The Dhala Structure, Bundelkhand craton, Central India—A new large Paleoproterozoic impact structure (abstract). *Meteoritics & Planetary Science* 40:A121.

Pati J. K., Reimold W. U., and Arvind 2006. Ballen quartz in impact melt rock from the Dhala impact structure, Bundelkhand craton, Central India (abstract), ESLAB-40: First International Conference on Impact Cratering in the Solar System, ESTEC, Noordwijk, The Netherlands. Abstract Book, pp.169–170.

Pati J. K., Raju S., Pruseth K. L., Malviya V. P., Arima M., Pati P., and Prakash K. 2007. Geology and geochemistry of giant quartz veins from the Bundelkahand craton, Central India and its implications. *Journal of Earth System Science* 116:497–510.

Prasad M. H., Hakim A., and Krishna Rao B. 1999. Metavolcanic and metasedimentary inclusions in the Bundelkhand Granitic Complex in Tikamgarh district, Madhya Pradesh. *Journal of the Geological Society of India* 54:359–368.

Rahaman A. and Zainuddin S. M. 1993. Bundelkhand granite: An example of collision-related Precambrian magmatism and its relevance to the evolution of the Central Indian Shield. *Journal of Geology* 101:413–419.

Rao K. V., Jain S. C., and Punekar D. V. 2005. Mohar cauldron—Geological and geophysical signatures (abstract). National Workshop on Mineral Deposit Modelling, South Asian Association of Economic Geologists, Nagpur. pp. 57–58.

Rao M. J., Rao P. G. V. S., Widdowson M., and Kelley S. P. 2005. Evolution of Proterozoic mafic dyke swarms of Bundelkhand craton, Central India. *Current Science* 88:502–506.

Ray J. S. 2006. Age of the Vindhyan Supergroup: A review of recent findings. *Journal of Earth System Science* 115:149–160.

Ray J. S., Veizer J., and Davis W. J. 2003. C, O, Sr, and Pb isotope systematics of carbonate sequences of the Vindhyan Supergroup, India: Age, diagenesis, correlation and implications for global events. *Precambrian Research* 121:103–140.

Reimold W. U. 2007. The Impact Cratering Bandwagon (Some problems with the terrestrial impact cratering record). *Meteoritics & Planetary Science* 42:1467–1472.

Reimold W. U., Koeberl C., and Bishop J. 1994. Roter Kamm impact crater, Namibia: Geochemistry of basement rocks and breccias. *Geochimica et Cosmochimica Acta* 58:2689–2710.

Reimold W. U., Trepmann C., and Simonson B. 2006. Discussion—Impact origin of the Ramgarh structure, Rajasthan: Some new evidences, by Sisodia et al. 2006. *Journal of the Geological Society of India* 68:561–563.

Sarangi S., Gopalan K., and Kumar S. 2004. Pb-Pb age of earliest megascopic eukaryotic alga-bearing Rohtas Formation, Vindhyan Supergroup, India: Implications for Precambrian atmospheric oxygen evolution. *Precambrian Research* 132:107–121.

Sarkar A., Paul D. K., and Potts P. J. 1996. Geochronology and geochemistry of mid-Archean trondhjemitic gneiss from the Bundelkhand craton, Central India. *Recent Researches in Geology* 16:76–92.

Short N. M. and Gold D. P. 1996. Petrography of shocked rocks from the central peak at the Manson impact structure, In: *The Manson impact structure, Iowa: Anatomy of an impact crater,* edited by Koeberl C. and Anderson R. R. GSA Special Paper 302. Boulder, Colorado: Geological Society of America. pp. 245–265.

Sisodia M. S., Lashkari G., and Bhandari N. 2006. Impact origin of the Ramghar structure, Rajasthan: Some new evidences. *Journal of the Geological Society of India* 67:423–431.

Srivastava S. K. and Nambiar K. V. 2003. '3-D' characterization of the Mohar cauldron, Shivpuri District, Madhya Pradesh. *Geological Survey of India Records* 136:52–54.

Srivastava S. K., Nambiar K. V., and Gaur V. P. 2002. Reconnaissance mapping of Bundelkhand Gneissic Complex in parts of Shivpuri, and Datia Districts, Madhya Pradesh with specialized thematic mapping in selected sectors. *Geological Survey of India Records* 135:64–66.

Stöffler D. and Langenhorst F. 1994. Shock metamorphism of quartz in nature and experiment: I. Basic observations and theory. *Meteoritics* 29:155–181.

Taylor S. R. and McLennan S. M. 1985. *The continental crust: Its composition and evolution.* Oxford: Blackwell. 312 p.

Turtle E. P., Pierazzo E., Collins G. S., Osinski G. R., Melosh H. J., Morgan J. V., and Reimold W. U. 2005. Impact structures: What does crater diameter mean? In *Large meteorite impacts III*, edited by Kenkmann T., Hörz F., and Deutsch A. GSA Special Paper 384. Boulder, Colorado: Geological Society of America. pp. 1–24.

Whitehead J., Spray J. G. and Grieve R. A. F. 2002. Origin of "toasted" quartz in terrestrial impact structures. *Geology* 30: 431–434.